Discovery of small molecule guanylyl cyclase B receptor positive allosteric modulators

Xiao Ma[a,1], Satyamaheshwar Peddibhotla [ID][b,1], Ye Zheng [ID][a], Shuchong Pan[a], Alka Mehta[b], Dante G. Moroni [ID][a], Qi-Yin Chen [ID][c], Xiaoyu Ma [ID][a], John C. Burnett Jr. [ID][a,d,*,2], Siobhan Malany [ID][b,*,2] and S. Jeson Sangaralingham [ID][a,d,*,2]

[a]Cardiorenal Research Laboratory, Department of Cardiovascular Medicine, Mayo Clinic, Rochester, MN 55905, USA
[b]Department of Pharmacodynamics, University of Florida, Gainesville, FL 32610, USA
[c]Department of Medicinal Chemistry, University of Florida, Gainesville, FL 32610, USA
[d]Department of Physiology and Biomedical Engineering, Mayo Clinic, Rochester, MN 55905, USA
*To whom correspondence should be addressed: Email: sangaralingham.jeson@mayo.edu (S.J.S.); Email: smalany@cop.ufl.edu (S.M.); Email: burnett.john@mayo.edu (J.C.B.)
[1]X.M. and S.P. contributed equally as first authors.
[2]J.C.B., S.M., and S.J.S. contributed equally as senior authors.
Edited By: J. Silvio Gutkind

Abstract

Myocardial fibrosis is a pathological hallmark of cardiovascular disease (CVD), and excessive fibrosis can lead to new-onset heart failure and increased mortality. Currently, pharmacological therapies for myocardial fibrosis are limited, highlighting the need for novel therapeutic approaches. The particulate guanylyl cyclase B (GC-B) receptor possesses beneficial antifibrotic actions through the binding of its natural ligand C-type natriuretic peptide (CNP) and the generation of the intracellular second messenger, cyclic guanosine 3′,5′-monophosphate (cGMP). These actions include the suppression of fibroblast proliferation and reduction in collagen synthesis. With its abundant expression on fibroblasts, the GC-B receptor has emerged as a key molecular target for innovative CVD therapeutics. However, small molecules that can bind and potentiate the GC-B/cGMP pathway have yet to be discovered. From a cell-based high-throughput screening initiative of the NIH Molecular Libraries Small Molecule Repository and hit-to-lead evolution based on a series of structure–activity relationships, we report the successful discovery of MCUF-42, a GC-B-targeted small molecule that acts as a positive allosteric modulator (PAM). Studies herein support MCUF-42's ability to enhance the binding affinity between GC-B and CNP. Moreover, MCUF-42 potentiated cGMP levels induced by CNP in human cardiac fibroblasts (HCFs) and notably also enhanced the inhibitory effect of CNP on HCF proliferation. Together, our findings highlight that MCUF-42 is a small molecule that can modulate the GC-B/cGMP signaling pathway, potentially enhancing the antifibrotic actions of CNP. Thus, these data underscore the continued development of GC-B small molecule PAMs as a novel therapeutic strategy for targeting cardiac fibrosis and CVD.

Keywords: guanylyl cyclase B receptor, cGMP, small molecule

Significance Statement

The particulate guanylyl cyclase B (GC-B) receptor, via its endogenous hormone C-type natriuretic peptide (CNP), plays a pivotal role in preventing the pathological manifestation of fibrosis in the heart. As such, peptide-based therapies to potentiate GC-B signaling are currently being developed. A major breakthrough in GC-B therapeutics would be a small molecule that sensitizes the GC-B receptor to endogenous CNP, which to date does not exist. Here, we report the discovery and development of a small molecule positive allosteric modulator of GC-B that exhibits therapeutic potential targeting myocardial fibrosis.

Introduction

Cardiovascular disease (CVD) is growing worldwide in which myocardial fibrosis is a hallmark pathologic characteristic of CVD (1–3). While myocardial fibrosis is an essential biological and reparative process that occurs in CVD, excessive accumulation of

cardiac fibrosis ultimately leads to heart failure (HF) and death (4, 5). However, current pharmacological therapies for myocardial fibrosis and the prevention of HF are limited and ultimately require a left ventricular assist device or heart transplantation. Thus, the discovery of novel drugs that specifically target aberrant

myocardial fibrosis would represent a major breakthrough in therapeutics for HF and CVD.

The particulate guanylyl cyclase B (GC-B) receptor signaling system, which functions via its endogenous ligand, C-type natriuretic peptide (CNP) and its second messenger, cyclic guanosine 3′,5′-monophosphate (cGMP), has been reported to be a potent fibro-inhibiting pathway (6–8). Indeed, studies have shown that the CNP/GC-B/cGMP pathway has robust antifibrotic actions that include the suppression of collagen synthesis, extracellular matrix deposition and fibroblast proliferation, inhibition of profibrotic cytokine [i.e. transforming growth factor-beta 1 (TGFβ1)] production, stimulation of endothelial cell growth, and vascular regeneration (6, 9–13). In the human heart, CNP is expressed in endothelial cells, cardiomyocytes, and fibroblasts (14), and clinical investigations have reported that CNP is significantly elevated in advanced atherosclerotic lesions (15, 16). In HF, a compensatory rise in circulating CNP has been reported (17, 18); however, this rise in CNP is suboptimal from an organ protection standpoint and therefore HF is a relative CNP deficiency state. Most importantly, supporting this pathway as a therapeutic target are studies that have reported that chronic subcutaneous or intravenous (IV) administration of CNP-based peptides results in a reduction in myocardial fibrosis and improved cardiac function (19, 20).

Moreover, recent studies by Werner et al. (21) have reported that mice with fibroblast-restricted deletion of the GC-B receptor had greater angiotensin II and left ventricular pressure overload-induced myocardial fibrosis compared to control mice, thus further supporting the importance of the fibro-inhibitory role of the GC-B receptor. The fibro-inhibiting significance of the CNP/GC-B/cGMP pathway sufficiently supports a rationale to develop novel therapeutics to enhance this protective system. One strategy along this line would be the development of CNP-based analogs, such as BMN-111 (also known as vosoritide), TransCon

CNP, or C53 (6, 22, 23), that are resistant to catabolism, unlike CNP which is rapidly degraded by neprilysin or cleared by the natriuretic peptide clearance receptor (NPRC) (24). However, the therapeutic potential of peptides has been largely limited by the major challenge of peptide instability and lack of oral administration.

The discovery of a small molecular compound that targets and enhances the GC-B/cGMP pathway, of which none exist to date, would represent a major therapeutic breakthrough in human therapeutics for myocardial fibrosis. Indeed, an emerging strategy in drug discovery has been the development of positive allosteric modulators (PAMs) which enhance the target receptor sensitivity to endogenous circulating and local tissue hormones (25–27). We recently reported the discovery of a GC-A receptor PAM, MCUF-651, which sensitizes the GC-A receptor to the endogenous cardiac hormones atrial natriuretic peptide (ANP) and b-type natriuretic peptide (28). Further, MCUF-651 was specific for the GC-A receptor and lacked any action on GC-B and, notably, is in preclinical development as a novel therapeutic strategy for hypertension.

The objective of the present study was to discover small-molecule enhancers or PAMs of the GC-B/cGMP pathway which would lay the foundation for novel GC-B-targeted antifibrotic therapies. Here, we describe the high-throughput screening (HTS) of the NIH Molecular Libraries Small Molecule Repository (MLSMR), medicinal chemistry, and structure–activity relationship (SAR) optimization studies which identified a lead GC-B PAM, MCUF-42. Furthermore, we designed the following investigations to evaluate the pharmacological and biological properties of MCUF-42 to: (i) enhance cGMP levels in HEK293 cells that overexpress GC-B or the alternative GC-A receptor, in order to determine its potency with the endogenous ligand of each receptor and its selectivity for the GC-B receptor; (ii) assess the binding of MCUF-42 alone, or in the presence of increasing concentrations of CNP, or with ANP, to human GC-B and GC-A, respectively; (iii) potentiate cGMP levels, in the presence of CNP, in human cardiac fibroblasts (HCFs); (iv) determine the pharmacokinetics (PK) and oral bioavailability of MCUF-42 in mice; and (v) enhance the antiproliferative effects mediated by CNP in HCFs, thus supporting its potential as an antifibrotic drug.
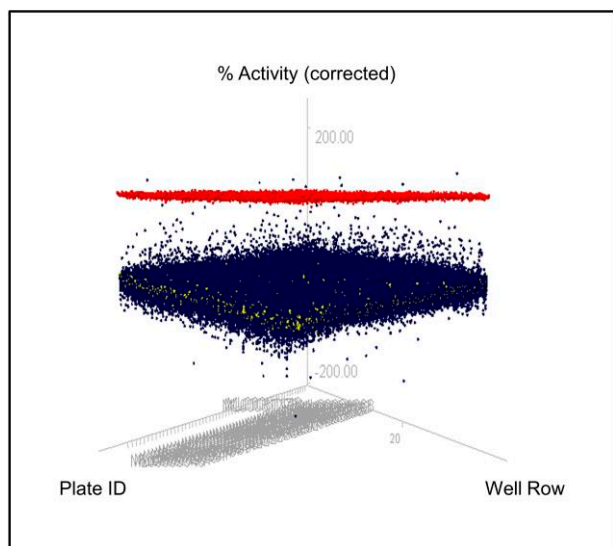

Fig. 1. HTS for GC-B potentiators. Scatter plot of percent activity for GC-B potentiators in the NIH MLSMR. Test compounds at 10 mM in the presence of 3 nM CNP are shown in blue. Negative control in the presence of 3 nM CNP (0% potentiation, CNP) is shown in yellow. Positive control in the presence of 300 nM CNP (100% potentiation) is shown in red. Compounds with >35% activity were considered hits in the screen. The Z′ for the assay was 0.87 with a signal to background of ~4.2 determined from the positive and negative control wells containing 300 and 3 nM CNP in 0.3% DMSO; respectively. The screening plates were normalized by GeneData pattern correction software.

Results

Discovery of small-molecule GC-B PAM scaffolds

We successfully screened the NIH MLSMR of 370,620 compounds (Fig. 1) in the presence of a subconcentration (3 nM in a 1,536-well screening assay) of CNP to sensitize the HTS toward detection of PAMs and identified 399 hits with >35% activity in the HEK293 cells expressing the GC-B receptor. Compound concentration–responses in the primary cell-based screening assay and a counter screen assay performed in parental HEK293 cells devoid of expressed GC-B receptor confirmed 199 compounds with GC-B activity. Of these, 106 compounds had activity >28% in HEK293 cells expressing the GC-A receptor. Finally, we identified 86 potential selective modulators of GC-B that had >28% activity at the target receptor and <28% activity at the GC-A receptor and at least >10% difference in activity between the two targets (Fig. S1). The hits were confirmed to be devoid of agonist activity in the absence of added CNP when tested in the HEK293 GC-B cells, thus, supporting their mode of action as PAMs. These compounds were graded according to activity, structure, and liability as potential pan-assay interference compounds resulting in 25 compounds that met

our internal criteria and were available as commercial powders (28, 29).

Hit confirmation studies

The active hits from primary screening were binned into 12 scaffolds, and commercially available analogs around these scaffolds were procured and assayed for potency as PAMs against GC-B/cGMP signaling assay in the presence of 3 nM CNP and selectivity versus GC-A/cGMP signaling assay in the presence of 3 pM ANP resulting in five chemical scaffolds which are available in PubChem (see Data Availability). One scaffold series was active in both GC-B and GC-A assays. As our primary focus was to identify enhancers that would specifically target GC-B, we deprioritized this scaffold series for the current study. We also deprioritized two other scaffold series because of weak activity toward GC-B, and they also had polycyclic fused ring systems, which has potential for poor solubility and other pharmacological properties. Notably, there were two scaffold series that were highly similar in structure, were active and selective toward GC-B, and thus were awarded the highest priority for synthesis and hit-to-lead SAR studies. Therefore, chemical stability, synthetic tractability, solubility, and complete dose–response and potency criteria led to the prioritization of the 5-aryl furan-2-thiocarboxamide and 5-aryl furan-2-carboxamide cores, respectively, represented by primary hit compound 1 (Fig. 2A). As illustrated in Fig. S2, compound 1 was specific in stimulating GC-B in the presence of an EC_{20} concentration of CNP and exhibited submicromolar potency and efficacy (0.74 μM and E_{max} of 112%; pEC_{50} of -6.6 ± 0.3, $n = 3$) compared to saturating concentrations of CNP. Further, compound 1 lacked activity in HEK293 GC-B cells when tested in the absence of CNP and also lacked activity in HEK293 GC-A cells in the presence of ANP up to 67 μM, thus supporting GC-B specificity and potentiation. Compound 1 has a robust and synthetically tractable structure and hence is a promising beginning point for synthesis of analogs and SAR studies in support of a focused hit-to-lead program.
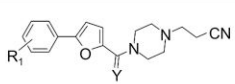
Hit-to-lead SAR studies

Compound 1, the primary hit, was resynthesized and recapitulated the activity of the commercial compound from the screening library (Fig. 2A, compound 1). Synthesis was modified from previously reported procedure based on Willgerodt–Kindler reaction (30) to access the key thioamide from the corresponding amine, furan-2-carboxaldehyde and elemental sulfur. Our synthesis was conducted under microwave irradiation (acetonitrile, 130 °C for 2 h) instead of thermal conditions. Replacement of thioamide with an amide resulted in complete loss of activity, demonstrating that thioamide is critical (compound 2). We next focused on aryl substitution at R1 position, based on synthesis of analogs from commercially available building blocks. Unsubstituted phenyl group (compound 3) resulted in ~8-fold loss of activity which could be dialed back with halogenated substituents, and 2-F, 3-Cl, and 4-Cl substituents resulted in equipotent analogs within 0.5–2.0× EC_{50} of primary hit 1. Next, we turned our attention to R2 substituents at the 1-position of the piperazine moiety. Having no substituent (R2 = H) or aryl and benzyl substituents at R2 led to inactive analogs (Fig. 2B, compounds 11–13). Surprisingly, N-acetyl piperazine analog was tolerated (compound 14). Replacement of the nitrile group from the propionitrile substituent in primary hit 1 with electron-rich methyl ether led to inactive compound 15. However, other electron-withdrawing substituents capable of forming H-bonds (donor) such as $-CO_2Et$ was tolerated (compound 17). Replacement of nitrile group in

compound 1 with 3-pyridinyl group led to inactive compound, whereas 2-pyridinyl substituent retained moderate activity (compounds 18 and 19). Compounds 16–19 highlight the requirement of specifically located (linker) of the small electron-withdrawing and H-bonding group at this position as a key driver of activity. Shortening the linker or having an acyl link between nitrile and piperazine moiety led to 2.5- to 3-fold loss of activity (compounds 20 and 21). We also examined some core replacements and found that replacement of furan ring with other heterocycles such as isoxazole and pyrazole led to complete loss of activity (Fig. 2C, compounds 22 and 23). We found that the piperidine analog 24 (Fig. 2C, compound 24) retained the potency of the piperazine-containing primary hit 1. Alkyl or acyl piperazines can have metabolic and potential toxic liabilities. Hence, compound 24 (referred to as MCUF-42) represents a significant change in structure from compound 1 and was not represented in the commercial space, but it retained equipotency. Hence, we decided to further evaluate the biological and PK properties of MCUF-42. The structure, procedure for synthesis, and characterization of MCUF-42 and analogs are described in Figs. S3–S6.

Biological profile of MCUF-42

The maximal GC-B receptor-mediated cGMP response was determined by saturating CNP levels (Fig. S7). MCUF-42 was identified as a selective GC-B PAM, as it was able to dose-dependently potentiate a subconcentration of CNP-induced cGMP with a potency of $EC_{50} = 0.80$ μM and $E_{max} = 86\%$ in HEK293 GC-B cells (Fig. 3A). MCUF-42 specifically increased cGMP levels by 4-fold in the presence of CNP (Fig. 3B). In the absence of CNP, MCUF-42 possessed no cGMP-generating activity in HEK293 GC-B cells (Fig. 3A and C). This absence of an agonist response further supports that MCUF-42 is modulating only the CNP target engagement with the GC-B receptor. Furthermore, and to confirm that the chemical series, represented by compound 1, retained selectivity to the GC-B receptor (Fig. S2), we observed that MCUF-42 lacked cGMP-producing activity in HEK293 GC-A cells in the presence of ANP (Fig. S8). To further characterize the mode of action as a GC-B PAM, we titrated CNP in the absence or presence of MCUF-42 (Fig. 3D). Increasing concentrations of MCUF-42 shifted the CNP-induced cGMP dose–response curve to the left, thus indicating increasing potency, with no additional enhancing effect on the maximal cGMP response. This confirms MCUF-42 is a PAM without agonistic activity. The EC_{50} value of CNP alone was 3.0 nM (in the 384-well dose–response assay), and the EC_{50} values of CNP in the presence of increasing concentrations of 0.157, 0.313, 0.625, 1.25, 2.5, and 5.0 μM MCUF-42 decreased to 1.4, 0.81, 0.70, 0.53, 0.37, and 0.31 nM, respectively, resulting in an overall 6.4-fold increase in affinity of CNP for GC-B when in the presence of 5.0 μM MCUF-42 compared to CNP by itself. From the data in Fig. 3D, we determined the change in the percent cGMP response of an EC_{30} concentration of the CNP (0.9 nM) curve in the absence of MCUF-42 ($logEC_{30} = -8.7 \pm 0.1$) to the CNP curves in the presence of increasing concentrations of MCUF-42. The percent cGMP response change of the EC_{30} concentration was plotted versus the corresponding concentration of MCUF-42 (Fig. 3E). This graph is referred to as the EC_{30} sensitivity assay. Nonlinear regression analysis of these data resulted in $pEC_{50} = -6.4 \pm 0.2$ ($EC_{50} = 0.36$ μM), which provides a quantitative assessment of intrinsic PAM affinity. In contrast, a less potent compound from our SAR studies, compound 22 ($EC_{50} > 10$ μM), showed no potentiation effects on cGMP activity in the presence of CNP in HEK293 GC-B cells
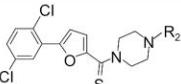
A

R1, aryl substitution

Compound	Y	R1	GC-B	
			EC$_{50}$ (µM)	E$_{max}$(%)
1 Primary hit	S	2,5-dichloro	0.79	137
2	0	2,5-dichloro	>10	–
3	S	H	6.41	60
4	S	2-F	1.57	96
5	S	2-Cl	2.33	75
6	S	2-CF3	>10	–
7	S	3-Cl	0.83	80
8	S	3-CF3	1.53	101
9	S	4-F	4.30	86
10	S	4-Cl	0.42	96
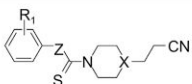
B

R2, N-cyanoethyl group replacements

Compound	R2	GC-B	
		EC$_{50}$ (µM)	E$_{max}$(%)
11	-H	>10	–
12	-Ph	>10	–
13	-CH$_2$Ph	>10	–
14	-COCH$_3$	2.90	95
15	-CH$_2$CH$_2$OCH$_3$	>10	–
16	-CH$_2$CH$_2$F	>8	–
17	-CH$_2$CH$_2$CO$_2$Et	2.53	73
18	-CH$_2$CH$_2$(2-pyridinyl)	1.20	148
19	-CH$_2$CH$_2$(3-pyridinyl)	>8	–
20	-CH$_2$C≡N	2.34	56
21	-COCH$_2$C≡N	1.99	62

C

Core replacements
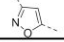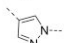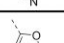
Compound	X	Z	R1	GC-B	
				EC$_{50}$ (µM)	E$_{max}$(%)
22	N	(isoxazole)	2,5-dichloro	>10	–
23	N	(pyrazole)	3-Cl	>8	–
24 MCUF-42	CH	(furan)	2,5-dichloro	0.80	86

Fig. 2. Structure–activity relationship studies and hit-to-lead development of 5-arylfuran-2-thioamide, MCUF-42. A) Hit synthesis, confirmation, and effect of aryl substitution at R1 position. B) Effect of N-cyanoethyl group replacements at R2 position. C) Effect of replacement of core furan and piperazine moieties in hit compound 1.

(Fig. S9). Altogether, we conclude that MCUF-42 is selective for the GC-B receptor and stimulated cGMP generation only in PAM mode.

Surface plasmon resonance (SPR) analysis was further conducted for the binding of MCUF-42 or CNP alone and MCUF-42 in the presence of increasing concentrations of CNP to the extracellular domain of human GC-B (Table 1). We confirmed the binding of MCUF-42 to human GC-B to have K_D of 710 nM. Strong binding of CNP to human GC-B was validated with a K_D of 0.17 nM. Importantly, the binding of CNP to GC-B was enhanced in the presence of MCUF-42 by a 2.6-fold increase in the association rate of the complex, thereby shifting the K_D (k_d/k_a) lower to 0.062 nM in the presence of MCUF-42 (5 µM). To support MCUF-42 as a GC-B PAM, we evaluated the binding of compound 22 that did not show potentiation effects on cGMP in our cell-based assay (Fig. S9). Our SPR studies demonstrated that binding compound 22 to the GC-B domain has a K_D of 558 nM; however, compound 22 did not alter the binding of CNP to GC-B as the K_D of CNP in the presence of compound 22 ($K_D = 0.16$ nM) remained similar to that of the binding of CNP alone to GC-B ($K_D = 0.14$). Together, these findings support that MCUF-42 binds to the GC-B receptor and enhances the affinity of CNP to the GC-B receptor.

In vivo PK and bioavailability in mice

In vivo PK studies in mice showed MCUF-42 (5 mg/kg) was bioavailable for 8 h when administered IV (Fig. S10). When given orally, MCUF-42 (10 mg/kg) exhibited limited absorption, but the compound was detectable for up to 2 h (Fig. S10). MCUF-42 showed oral bioavailability of 0.26% (Table S1).

In vitro cGMP generation of MCUF-42 in human cardiac fibroblasts

We further investigated the ability of MCUF-42 to enhance the cGMP generation of CNP in HCFs. Consistent with the potency observed in HEK293 GC-B cells, adding increasing concentrations (1, 5, and 10 µM) of MCUF-42 on top of CNP at a dose of 100 pM, a low experimental dose close to the plasma concentrations of CNP in humans under physiological conditions significantly enhanced cGMP generation in HCFs (Fig. 4A).

In vitro inhibition of human cardiac fibroblasts proliferation with MCUF-42

A key property of the GC-B/cGMP signaling pathway is its antifibrotic actions within the heart under pathophysiological stress. To further define the therapeutic potential of MCUF-42 on this aspect, we evaluated the MCUF-42's ability to enhance the antifibrotic actions of the GC-B natural ligand, CNP, in HCFs stimulated by the potent fibrotic cytokine TGFβ1. Here, we utilized the inhibition of HCF proliferation as the primary endpoint which was performed via live-cell, time-lapsed imaging. In the absence of CNP, there was no suppression of TGFβ1-stimulated HCF proliferation with MCUF-42 (Fig. S11). However, MCUF-42 at concentrations of 5 µM ($P < 0.0001$) and 10 µM ($P = 0.0019$) (Fig. 4B), together
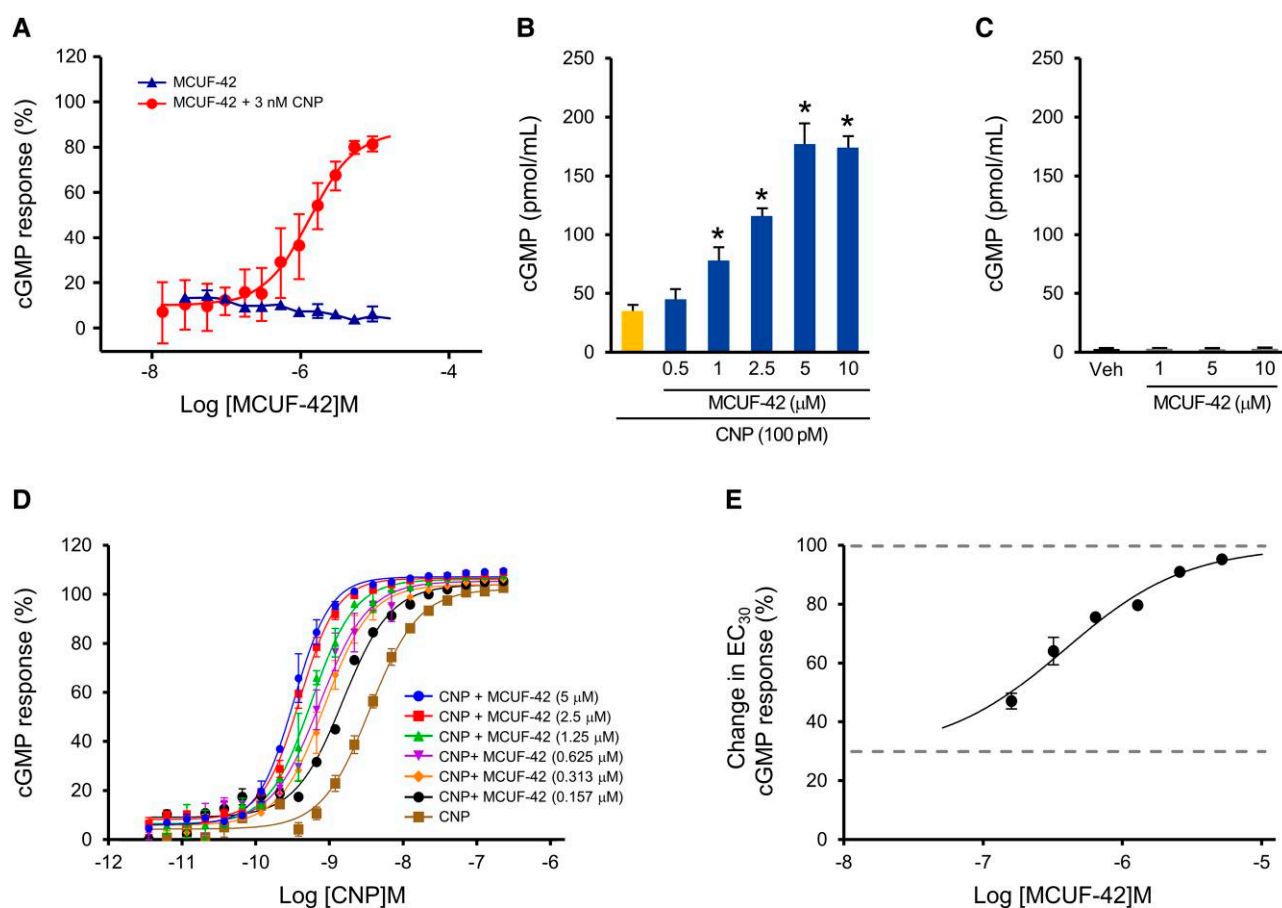
Fig. 3. Activity of MCUF-42 in HEK293 GC-B cells. A) Percent cGMP concentration–response curves for cGMP response with increasing doses of MCUF-42 (blue) and increasing doses of MCUF-42 in the presence of 3 nM CNP (red) in HEK293 GC-B cells. B) cGMP generation of CNP alone (yellow bar) and CNP in the presence of MCUF-42 (blue bars) in HEK293 GC-B cells. C) cGMP generation of vehicle alone (black bar) or MCUF-42 alone (gray bars) in HEK293 GC-B cells. D) Percent cGMP concentration–response curves in HEK293 GC-B cells for CNP titrated alone (brown) and CNP titrated together with increasing concentrations of MCUF-42. E) Change in cGMP concentration–response for the EC_{30} concentration of CNP determined in (D) in the presence of increasing concentrations of MCUF-42. The line fits are nonlinear regression analysis of the data. In A), D), and E), data are presented as mean ± SD. In B) and C), data are presented as mean ± SEM. In B), one-way ANOVA with post hoc Tukey's test was used to determine the inter-group difference with *indicating $P < 0.05$ compared to the CNP alone group (yellow bar).

Table 1. SPR-binding kinetics for MCUF-42 and CNP to the human GC-B receptor.

	k_a (M^{-1}s^{-1})	k_d (s^{-1})	K_D (nM)
MCUF-42	8.4×10^4	5.9×10^{-2}	710
CNP	2.1×10^8	3.5×10^{-2}	0.17
MCUF-42 + CNP	5.4×10^8	3.3×10^{-2}	0.062

MCUF-42 alone binds to GC-B. MCUF-42 (5 μM) further enhanced the binding affinity of CNP to GC-B by increasing the association rate, thus reducing the equilibrium dissociation rate. k_a, association rate; k_d, dissociation rate; K_D, equilibrium dissociation rate.

with CNP (100 pM), significantly inhibited TGFβ1-stimulated HCF proliferation compared to CNP alone.

Discussion

Herein, we report the first study in exploring small molecule PAMs targeting the GC-B receptor. Specifically, we highlight, from a HTS campaign of the NIH MLSMR and extensive hit-to-lead evolution based on a series of SARs, the successful discovery and engineering of MCUF-42, a GC-B-targeted small molecule that acts as a PAM. Notably, we have demonstrated the biological actions of MCUF-42 on the GC-B/cGMP system. First, MCUF-42 enhances cGMP levels stimulated by CNP in HEK293 GC-B cells. Second, MCUF-42 enhances the binding between GC-B and its natural ligand, CNP. Third, MCUF-42 potentiates cGMP levels stimulated by CNP in HCFs. Lastly, MCUF-42 enhances CNP mediated inhibition of HCF proliferation triggered by profibrotic TGFβ1. Altogether, our study supports further developing MCUF-42 as a selective GC-B small molecule drug targeting myocardial fibrosis.

The GC-B/cGMP signaling pathway has grown to be an attractive target for the treatment of CVD because its activation, with CNP or CNP-based analogs, leads to cardiac protection with its potent antifibrotic actions (6, 11, 19–21). While CNP-based therapeutics represents a unique class of biopharmaceuticals that continues to evolve in drug discovery, they have challenges with peptide instability and oral delivery. Thus, the discovery and development of small molecules that target and enhance the GC-B/cGMP pathway would be a pivotal therapeutic advancement.

We and others have reported the discovery of novel small molecules that target the GC-A or GC-B receptor (28, 31, 32). These small molecules include enhancers of GC-A through positive allosteric modulation (28, 32) or antagonists of GC-B (31). However and to our knowledge, a small molecule that can engage and
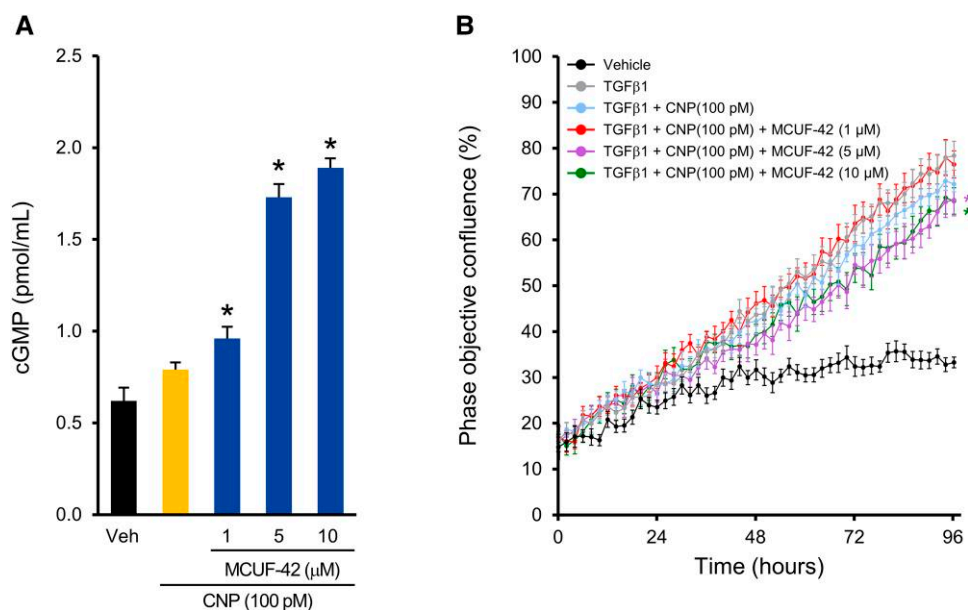
Fig. 4. Biological actions of MCUF-42 on CNP in human cardiac fibroblasts. A) Generation of cGMP in HCFs stimulated by CNP (100 pM) alone or in the presence of 1, 5, and 10 µM MCUF-42. B) Inhibition of TGFβ1-induced HCF proliferation by CNP (100 pM) alone or in the presence of 1, 5, and 10 µM MCUF-42. Data are presented as mean ± SEM. In A), one-way ANOVA with post hoc Tukey test was used to determine the inter-group difference with * indicating $P < 0.05$ compared to the CNP alone group (yellow bar). In B), two-way ANOVA with post hoc Tukey test was used to determine the main group effect with * indicating $P < 0.05$ compared to TGFβ1 + CNP group (light blue line).

enhance the GC-B receptor has yet to be discovered. Therefore, our HTS efforts employing the NIH MLSMR and targeting the GC-B/cGMP system, in the presence of a low concentration of the natural ligand, represent a strategic approach for small molecule allosteric modulator drug discovery. From our screening efforts, we did not identify any small molecules that would serve as agonists of the GC-B/cGMP system. However, we identified a promising hit compound that acts as a selective GC-B-targeted PAM. Medicinal chemistry and SAR-based optimization studies on the screening hits led to the identification of a lead GC-B PAM, MCUF-42. In line with our previous discovery of the GC-A PAM MCUF-651, our discovery of MCUF-42 and findings reiterate important allosteric binding sites on particulate GC receptors which have the ability to bind PAMs and enhance the effects of GC ligands that bind to the orthosteric site of the receptor. Indeed, PAMs have unique advantages over orthosteric-interacting molecules including not competing for the same binding site as the ligand, are potentially safer as they require ligand binding to be effective, and thus avoid overstimulation of the receptor, and allosteric sites are generally less conserved which allows for the opportunity to selectively target specific subfamily of receptors (25–27, 32).

The second messenger, cGMP, is the central intracellular signaling molecule which mediates the protective actions of the GC-B receptor upon activation. Its elevation is a reliable and well-recognized index to identify target engagement and to quantify the activation of the GC-B receptor. In current study, we demonstrated that MCUF-42 dose-dependently enhanced CNP-mediated cGMP production in the HEK293 GC-B cells and exhibited no cGMP-generating actions in the absence of CNP. Furthermore, MCUF-42 had no effect on cGMP production in the HEK293 GC-A cells in the presence of ANP, thus establishing MCUF-42 as a GC-B receptor-specific PAM. These findings were further corroborated with SPR-binding studies. Our binding studies demonstrated that MCUF-42 binds to the extracellular domain of the GC-B receptor; however, it has >1,800-fold less affinity than the GC-B ligand,

CNP. Notably in the presence of CNP, MCUF-42 enhanced the binding affinity of CNP to GC-B by increasing the association rate, thus reducing the equilibrium dissociation rate. It is tempting to speculate that MCUF-42 binds to an allosteric site on the extracellular domain of GC-B, thus triggering a favorable receptor conformational change which in turn enhances the ability of CNP to engage the binding pocket more effectively. Our SPR data suggest that it is the faster association rate and greater target engagement, which lower the energy of activation, that is driving the increase in potency of GC-B peptide ligand, CNP, in the presence of MCUF-42. This paradigm in regulating GC-B receptor activity, with a PAM, provides new scientific insight into GC-B enhancement which has important therapeutic implications.

The GC-B/cGMP signaling pathway has been reproducibly reported as a potent inhibitor of organ fibrosis in various experimental models of CVDs as well as kidney and lung injury or disease (10, 19, 33, 34). Cardiac fibrosis, in particular, is a progressive process that leads to HF and mortality for which there are no effective or FDA-approved drugs (2, 3, 5). Thus, enhancing or augmenting the GC-B/cGMP system may represent a novel therapeutic opportunity to reduce myocardial fibrosis. To further support the therapeutic potential, particularly in targeting cardiac fibrosis, of GC-B enhancement with the PAM MCUF-42, we investigated the cGMP-generating actions on HCFs, which naturally express an abundance of GC-B receptors (35). Consistent with our findings in HEK293 cells, we found that MCUF-42 can enhance the cGMP production mediated by CNP in a dose-dependent manner in HCFs. We then extended these findings to a functional assay where we investigated the antifibrotic action of MCUF-42 in HCFs, in the presence of a low dose of CNP. Importantly, we mimicked a potential pathophysiological environment by stimulating HCFs proliferation with TGFβ1, an important driver of cardiac fibrosis which is activated with cardiovascular injury and CVD. The key finding is that a pharmacological treatment with MCUF-42 in the presence of CNP enhanced the attenuation of

TGFβ1-induced HCFs proliferation over 96 h compared to CNP alone. Together, these findings support the therapeutic potential of MCUF-42, a GC-B PAM, for targeting myocardial fibrosis. Further in vitro and in vivo investigations are needed to confirm and validate these novel findings. While the CNP/GC-B/cGMP has classically been the pathway that has been attributed to the favorable antifibrotic actions in the heart (6, 19, 21), emerging evidence has also suggested that CNP may mediate antifibrotic actions in the heart via NPRC and non-cGMP-mediated signaling (36, 37). Thus, future studies are warranted to investigate whether MCUF-42 alters CNP and NPRC signaling or clearance, which could illuminate alternative mechanisms that complement its established cGMP-mediated benefits through GC-B in mitigating cardiac fibrosis.

The therapeutic delivery strategy for natriuretic peptides and novel bioengineered analogs has been predominantly limited to IV or subcutaneous administration (38–46). Accordingly, we have evaluated the PK of MCUF-42 given as an IV bolus in conscious mice. We found MCUF-42 is detectable in circulation up to 8 h postbolus examination, suggesting a much longer half-life of MCUF-42 compared to GC-B peptide ligands including CNP and its analogs. Another major advantage of small molecules over peptides is the relative ease for oral delivery. Based upon the chemical characteristics of MCUF-42, we also determined the bioavailability of oral delivery in conscious mice. Herein, we observed that MCUF-42 is orally bioavailable, albeit very modestly, and further optimization is needed to increase the absorption and bioavailability via oral administration.

In summary, we report the discovery and development of a small-molecule GC-B PAM that is active in HCFs and exhibits therapeutic potential in preventing and/or reducing cardiac fibrosis by potentiating the GC-B-mediated second messenger, cGMP. These studies provide scientific evidence that supports the concept that GC-B based therapy can be achieved via a small molecule PAM in addition to the traditional peptide approach. Thus, this discovery may be game-changing and accelerate the translation of GC-B-targeted therapeutics for cardiac fibrosis as seen with CVDs.

Materials and methods
Peptides and compounds

Human CNP (Phoenix Pharmaceutical, Burlingame, CA, USA) was dissolved in water at 500 mM stock and aliquoted and stored at −20 °C. Compound 1 (CAS# 332862-27-8) was purchased from LifeChem (F1813-1161, Woodbridge, CT, USA). Compound 1 was resynthesized, and analogs were prepared at University of Florida according to the representative procedure (Fig. S3) or at BioDuro-Sundia, China. MCUF-42 was scaled up for PK studies at Jubilant Biosys Limited (Bengaluru, India). All other chemicals and reagents were obtained from Sigma-Aldrich (St Louis, MO, USA). The identity and purity of MCUF-42 were confirmed using H^1-NMR, liquid chromatography–mass spectrometry (LC–MS) trace, and mass spectrometry (MS) spectrum (Figs. S4–S6).

Cell culture for HTS

HEK293 cells overexpressing human GC-B (Cardiorenal Research Laboratory, Mayo Clinic, Rochester, MN, USA) and the parental cell line (ATCC CRL-1573) devoid of either GC-B or GC-A were cultured in growth media consisting of Dulbecco's modified Eagle medium (Corning; no. 10013CM) containing 1% L-glutamine and sodium pyruvate and supplemented with 10% fetal bovine serum

(FBS; HyClone; SH30396.03) and 500 μg/mL of G418 (Thermo Fisher; no. 10131035), as previously described (28). Cell culture was maintained in a cell culture incubator at 37 °C in 5% CO_2 and routinely subcultured twice weekly by trypsin–ethylenediaminetetraacetic acid (EDTA) treatment (0.25% trypsin–EDTA). On the day of the assay, the cells were thawed, counted, and resuspended in assay media (OptimMem containing 2% heat-activated FBS and 1% L-glutamine) and used as described in HTS cGMP production. The human GC-A and GC-B receptor expression in HEK293 overexpressing and parental cells has been verified by western blotting as previously reported (47).

HTS cGMP production

In our effort to identify GC-B PAMs from the NIH MSMLR, we used a similar procedure as we have previously described for targeting the GC-A receptor (28). In brief, we monitored production of cGMP, the second messenger generated by GC-B activation, by homogenous time-resolved florescence (HTRF) competition assay using labeled cGMP in HEK293 cells overexpressing the human GC-B receptor. Compound EC_{50} values were determined by the primary cell-based screening assay, in the presence or absence of CNP, to determine mode of action as positive modulators and tested for selectivity in the same assay platform but in HEK293 cells overexpressing human GC-A, for which ANP is the endogenous ligand and not CNP.

For HTS, GC-B suspension cells were plated in 1,536 wells and stimulated in the presence of 10 μM compound concentration and a submaximal concentration of CNP. The quantity of cGMP was detected by HTRF and normalized to maximal amount produced by CNP. Specifically, 20 nL of 10 mM test compounds in dimethyl sulfoxide (DMSO) from the NIH MLSMR (370,620 test compounds) was added to columns 5–48 of 1,536-well white high base screening plates (Corning, New York, NY, USA) cells using a 550 Echo acoustic dispenser (Labcyte, San Jose, CA, USA). CNP was prepared as working stock aliquots at 5 mM in phosphate buffered saline (PBS) with 0.1% bovine serum albumin (BSA). An approximate EC_{30} concentration of CNP (3 nM) in assay buffer (Hanks' balanced salt solution [HBSS] containing 5 mM 4-(2-hydroxyethyl)-1-piperazineethanesulfonic acid [HEPES] and 0.05% BSA) was added to columns 3–48 at a volume of 1 μL. Assay buffer only was added to column 1, while assay buffer containing a saturating concentration of CNP (300 nM) was added to column 2. HEK293 cells overexpressing human GC-A in assay media were stirred continuously for 2 h at room temperature (RT) at a density of 6×10^5 cells/mL, and 2 μL was plated in screening plates (1,200 cells/well) using a BioRaptr 2. Plates were spun at 1,000 rpm for 1 min and incubated for 30 min at RT. 1.5 μL of d2-labled cGMP followed by 1.5 μL of Eu3+ cryptate-labeled anti-cGMP cGMP detection kit (CiBio; #62GM2PEC) prepared according to the manufacturer's protocol was added to all wells using a BioRaptr 2, and time-resolved fluorescence resonance energy transfer (TR-FRET) signal was detected on an EnVision detector (PerkinElmer). Wells treated with 0.3% DMSO served only as blank controls (column 1); wells treated with 0.3% DMSO and 300 nM CNP (columns 2) served as positive controls; and wells treated with 0.3% DMSO and 3 nM CNP (columns 3 and 4) served as negative controls. DMSO did not exceed 0.3% in all wells.

EC_{50} cGMP determination

Compound EC_{50} values were determined by the primary cell-based screening assay as we previously reported (28), however, in this study, in the presence or absence of CNP, to determine

mode of action as positive modulators. Test compounds at 10 mM DMSO stock concentration were added to 384-well assay plates using Tecan dispensing starting at 8 µM concentration and diluted 2-fold for 10-point concentration–response curves. Wells were backfilled with DMSO such that the final concentration of DMSO in all wells was maintained at 0.3% DMSO. Wells with compounds were stimulated with an EC_{30} concentration of CNP. The quantity of cGMP was detected by HTRF and normalized to maximal amount produced by CNP. An approximate EC_{30} concentration of CNP (1 nM) in assay buffer (HBSS containing 5 mM HEPES and 0.05% BSA) was added to columns 3 to 48 at a volume of 10 µL. Assay buffer only was added to column 1, while assay buffer containing a saturating concentration of CNP (100 nM) was added to column 2. HEK293 cells overexpressing human GC-B in assay media were stirred continuously at RT at a density of 2×10^6 cells/mL, and 10 µL was plated in screening plates (5,000 cells/well) using a VIAFLO-multichannel pipette. Plates were spun at 1,000 rpm for 1 min and incubated for 30 min at RT. A 5 µL of d2-labled cGMP followed by 5 µL Eu3+ cryptate-labeled anti-cGMP cGMP detection kit (CiBio; #62GM2PEC) prepared according to the manufacturer's protocol was added to all wells using a VIAFLO-multichannel pipette, and TR-FRET signal was detected on a ClarioStar Plus plate reader (BMG-Labtech). Wells treated with 0.3% DMSO served only as blank controls (column 1), wells treated with 0.3% DMSO and 50 nM CNP (columns 2) served as positive controls, and wells treated with 0.3% DMSO and 1 nM CNP (columns 3 to 4) served as negative controls. DMSO did not exceed 0.3% in all wells. A 0% response was determined from wells containing an EC_{20} concentration of CNP. A 100% response was determined from wells in the presence of saturating concentration of CNP ($EC_{80} = 100$ nM). This concentration of CNP was less than that used in the HTS and provided a sufficient signal to background window and lowered the amount of material needed. Since the HTS is optimized for stability over time, a higher CNP concentration was employed during HTS. 100–300 nM was in the EC_{80}–EC_{100} saturation range.

cGMP levels in HEK293 cells overexpressing human GC-B or GC-A receptor

HEK293 GC-B or GC-A cells were seeded at 10^5 cells/well in 48-well plates and cultured overnight to reach 80–90% confluency as we have performed previously (6, 28). In all experiments, a treatment buffer which consists of HBSS, 0.5 mM 3-isobutyl-1-methylzanthine (IBMX, a nonspecific inhibitor of phosphodiesterase), 2 mM HEPES, and 0.1% BSA was used. On the day of experiment, HEK293 GC-B or GC-A cells were pretreated with MCUF-42 at doses of 0.5, 1, 2.5, 5, and 10 µM for 5 min at 37 °C. The culture medium was then replaced by the treatment buffer containing 100 pM CNP (for HEK293 GC-B cells) or 100 pM ANP (for HEK293 GC-A cells) and incubated at 37 °C for additional 10 min. After the treatment, cells were washed once with PBS and lysed with 0.1 M HCl. The intracellular cGMP was measured in the lysate using a cGMP ELISA Kit (Enzo Life Sciences) following the manufacturer's instructions and a similar fashion as other studies (6, 28).

cGMP levels in human primary cardiac fibroblasts

HCFs (catalog # 12375, lot # 424Z011.9, PromoCell, Heidelberg, Germany) were maintained and subcultured according to the manufacturer's protocols and as described in other studies (6). Cells at passage 4 were used in the current study. Briefly, HCFs were cultured in 6-well plates until 80% confluency before being treated with treatment buffer (same as in HEK293 cell experiments) alone, with 100 pM CNP alone, or with 100 pM CNP and

different concentrations (1, 5, and 10 µM) of MCUF-42 for 10 min. After the treatment, cells were washed once with PBS and lysed with 0.1 M HCl. The intracellular cGMP was measured in the lysate using a cGMP ELISA Kit (Enzo Life Sciences) following the manufacturer's instruction and a similar fashion as other studies (6, 28).

Live cell, real-time human cardiac fibroblasts proliferation imaging and analysis

HCFs (same as above) proliferation assay was performed using the automated live-cell, real-time imaging and analysis IncuCyte Zoom system (Essen BioScience, Ann Arbor, MI, USA) as described previously (6). HCF proliferation was monitored by time-lapse imaging and analyzed by the IncuCyte Zoom system software, enabling determination of cell density (% confluence) over time. Briefly, HCFs were seeded at 1.5×10^4 cells/well in a 96-well plate and cultured in fibroblast growth medium 3 (catalog # 23025, PromoCell, Heidelberg, Germany) with 10% FBS for 24 h without starvation. The cells, in fibroblast growth media 3 without IBMX, were then treated with PBS (vehicle) alone, 5 ng/mL of the profibrotic cytokine TGFβ1 (R&D Systems, Minneapolis, MN, USA) alone, TGFβ1 (5 ng/mL) together with 1, 5, and 10 µM of MCUF-42, TGFβ1 (5 ng/mL) together with CNP (100 pM), or TGFβ1 (5 ng/mL) together with CNP (100 pM) and different concentrations (1, 5, and 10 µM) of MCUF-42. Phase-contrast images were taken continuously for 4 days as instructed by the manufacturer, and data images were analyzed using the corresponding software. The effect of MCUF-42 (on top of CNP) on HCFs proliferation was compared to the CNP alone group.

GC-B binding studies

SPR measurements were taken at 25 °C on a BI-4500 SPR instrument (Biosensing Instrument Inc.) to determine binding as previously reported with modifications (28). As per the instructions by the Biosensing Instrument manual, 400 mM nickel sulfate in deionized water was linked to the Ni-NTA sensor chip (Biosensing Instrument Inc.). The extracellular domain of human GC-B recombinant protein (MyBioSource Inc.) at the concentration of 40 µg/mL was then immobilized to the nickel sulfate on the Ni-NTA sensor chip. Afterward, the chip was washed with buffer (150 mM NaCl, 50 µM EDTA pH 7.4, 0.1% DMSO) followed by the injection of 100 µL of sequentially diluted MCUF-42 (0.31, 0.625, 1.25, 2.5, and 5 µM) alone at the rate of 60 µL/min which was allowed to dissociate for 60 s. For GC-B binding studies with CNP, 100 µL of sequentially diluted CNP (0.0625, 0.125, 0.25, 0.5, and 1 nM) alone or CNP (0.0625, 0.125, 0.25, 0.5, and 1 nM) together with MCUF-42 (5 µM) was injected at the rate of 60 µL/min and allowed to dissociate for 200 s. Similar experiments were performed with compound 22. All data were collected as sensorgrams, and the binding kinetics were derived from sensorgrams using the BI-Data Analysis Program (Biosensing Instrument Inc.). Affinity analysis of GC-B with CNP and/or MCUF-42 interactions was performed using a 1:1 Langmuir binding model. Two series of experiment were performed for all studies.

PK studies

All procedures used for the PK studies were performed at Jubilant Biosys Limited and approved by its Institutional Animal Care and Use Committee under protocol number IAEC-JDC-2021-257R. The PK of MCUF-42 was investigated in male Balb/C mice (Vivo Biotech, Hyderabad, India, 6–8 weeks old, 23–26 g) using a sparse sampling design. A total of 24 mice were used and divided into

two groups to receive one of the following treatments, a single dose of 5 mg/kg IV and 10 mg/kg orally [per os (PO)] by gavage. The mice were fed food and water ad libitum throughout the study for IV group, while for PO group mice were kept for 4-h fasting before dosing and food was provided 2 h post dose with water ad libitum. The vehicle used was Tween-80 and 0.5% methyl cellulose (0.5:99.5; v/v) in Milli-Q water for PO dosing, and DMSO, solutol/ethanol (1:1), and normal saline (10:10:80 v/v) were used for IV dosing. Two aliquots of each (IV and PO) formulation were dose-validated by high-performance liquid chromatography. All blood samples were transferred to a microcentrifuge tube containing 5 µL of 10% K_2EDTA (0.5 mL) as an anticoagulant agent and placed on ice until processed for plasma. Blood samples were processed for plasma by centrifugation at 10,000 rpm for 5 min at 4 °C, quickly frozen, and stored at −80 °C until quantification by LC–MS/MS.

Statistical analysis and regression curve fitting

All concentration–response curves were analyzed to determine EC_{50} and E_{max}. All E_{max} values were calculated using the equation $E_{max} = 100/[1 + 10^{(LogEC50-X)*Hill\text{-}slope}]$, where X is the log of the tested compound concentration and the Hill-slope is set to be 1. For concentration–response data, nonlinear regression curve fitting, and statistical analyses were performed using Prism 9 (GraphPad Software Inc.), and $P < 0.05$ was considered as statistically significant. All presented experimental data related to cells and mice studies were acquired in at least three biological replicates ($n \geq 3$). Unless specified otherwise, all numeric data are expressed as mean ± SEM or SD. Unpaired t test assuming unequal variance was performed for the comparison between each pair of two groups in HEK293 cells and HCFs. One-way or two-way analysis of variance (ANOVA) was used for the comparison among multiple groups followed by post hoc multiple comparisons using Tukey's method. For the PK studies, plasma concentration data were analyzed with standard noncompartmental analysis with the Phoenix WinNonlin software (8.1 version, Copyright © 2023, Certara, USA). Mean plasma concentration–time profiles were constructed for PK analysis in the mouse. The systemic CL and the steady-state volume of distribution and half-life were calculated after IV administration, and the C_{max}, T_{max}, and area under the curve (AUC) values were calculated using a combination of linear trapezoidal and linear interpolation summations. The absolute oral bioavailability (%) was estimated by taking the ratio of dose-normalized AUC values.

Supplementary Material

Supplementary material is available at *PNAS Nexus* online.

Data Availability

The data supporting the findings presented in this manuscript are included in the main article, supplementary material, and/or PubChem. The primary assay data and protocols from the HTS are available at PubChem under the Assay ID: 1920062.

References

1   Mensah GA, Roth GA, Fuster V. 2019. The global burden of cardiovascular diseases and risk factors: 2020 and beyond. *J Am Coll Cardiol*. 74:2529–2532.

2   Rockey DC, Bell PD, Hill JA. 2015. Fibrosis—a common pathway to organ injury and failure. *N Engl J Med*. 372:1138–1149.

3   Travers JG, Kamal FA, Robbins J, Yutzey KE, Blaxall BC. 2016. Cardiac fibrosis: the fibroblast awakens. *Circ Res*. 118:1021–1040.

4   Tsao CW, *et al.* 2023. Heart disease and stroke statistics—2023 update: a report from the American Heart Association. *Circulation*. 147:e93–e621.

5   Gonzalez A, Schelbert EB, Diez J, Butler J. 2018. Myocardial interstitial fibrosis in heart failure: biological and translational perspectives. *J Am Coll Cardiol*. 71:1696–1706.

6   Chen Y, *et al.* 2019. C53: a novel particulate guanylyl cyclase B receptor activator that has sustained activity in vivo with antifibrotic actions in human cardiac and renal fibroblasts. *J Mol Cell Cardiol*. 130:140–150.

7   Michel K, *et al.* 2020. C-type natriuretic peptide moderates titin-based cardiomyocyte stiffness. *JCI Insight*. 5:e139910.

8   Sangaralingham SJ, Kuhn M, Cannone V, Chen HH, Burnett JC. 2023. Natriuretic peptide pathways in heart failure: further therapeutic possibilities. *Cardiovasc Res*. 118:3416–3433.

9   Yamahara K, *et al.* 2003. Significance and therapeutic potential of the natriuretic peptides/cGMP/cGMP-dependent protein kinase pathway in vascular regeneration. *Proc Natl Acad Sci U S A*. 100:3404–3409.

10 Kimura T, *et al.* 2016. C-type natriuretic peptide ameliorates pulmonary fibrosis by acting on lung fibroblasts in mice. *Respir Res*. 17:19.

11 Ichiki T, *et al.* 2014. Cardiac fibrosis in end-stage human heart failure and the cardiac natriuretic peptide guanylyl cyclase system: regulation and therapeutic implications. *J Mol Cell Cardiol*. 75:199–205.

12 Horio T, *et al.* 2003. Gene expression, secretion, and autocrine action of C-type natriuretic peptide in cultured adult rat cardiac fibroblasts. *Endocrinology*. 144:2279–2284.

13 Doi K, *et al.* 2001. C-type natriuretic peptide induces redifferentiation of vascular smooth muscle cells with accelerated reendothelialization. *Arterioscler Thromb Vasc Biol*. 21:930–936.

14 Chaffin M, *et al.* 2022. Single-nucleus profiling of human dilated and hypertrophic cardiomyopathy. *Nature*. 608:174–180.

15 Casco VH, *et al.* 2002. Natriuretic peptide system gene expression in human coronary arteries. *J Histochem Cytochem*. 50:799–809.

16 Naruko T, *et al.* 1996. C-type natriuretic peptide in human coronary atherosclerotic lesions. *Circulation*. 94:3103–3108.

17 Ma X, *et al.* 2021. Prognostic value of urinary and plasma C-type natriuretic peptide in acute decompensated heart failure. *JACC Heart Fail.* 9:613–623.

18 Lok DJ, *et al.* 2014. Prognostic value of N-terminal pro C-type natriuretic peptide in heart failure patients with preserved and reduced ejection fraction. *Eur J Heart Fail.* 16:958–966.

19 Soeki T, *et al.* 2005. C-type natriuretic peptide, a novel antifibrotic and antihypertrophic agent, prevents cardiac remodeling after myocardial infarction. *J Am Coll Cardiol.* 45:608–616.

20 Martin FL, *et al.* 2012. CD-NP: a novel engineered dual guanylyl cyclase activator with anti-fibrotic actions in the heart. *PLoS One.* 7:e52422.

21 Werner F, *et al.* 2023. Ablation of C-type natriuretic peptide/cGMP signaling in fibroblasts exacerbates adverse cardiac remodeling in mice. *JCI Insight.* 8:e160416.

22 Wendt DJ, *et al.* 2015. Neutral endopeptidase-resistant C-type natriuretic peptide variant represents a new therapeutic approach for treatment of fibroblast growth factor receptor 3-related dwarfism. *J Pharmacol Exp Ther.* 353:132–149.

23 Breinholt VM, *et al.* 2019. TransCon CNP, a sustained-release C-type natriuretic peptide prodrug, a potentially safe and efficacious new therapeutic modality for the treatment of comorbidities associated with fibroblast growth factor receptor 3-related skeletal dysplasias. *J Pharmacol Exp Ther.* 370:459–471.

24 Hunt PJ, Richards AM, Espiner EA, Nicholls MG, Yandle TG. 1994. Bioactivity and metabolism of C-type natriuretic peptide in normal man. *J Clin Endocrinol Metab.* 78:1428–1435.

25 Wenthur CJ, Gentry PR, Mathews TP, Lindsley CW. 2014. Drugs for allosteric sites on receptors. *Annu Rev Pharmacol Toxicol.* 54:165–184.

26 Abdel-Magid AF. 2015. Allosteric modulators: an emerging concept in drug discovery. *ACS Med Chem Lett.* 6:104–107.

27 Christopoulos A. 2002. Allosteric binding sites on cell-surface receptors: novel targets for drug discovery. *Nat Rev Drug Discov.* 1:198–210.

28 Sangaralingham SJ, *et al.* 2021. Discovery of small molecule guanylyl cyclase A receptor positive allosteric modulators. *Proc Natl Acad Sci U S A.* 118:e2109386118.

29 Baell JB, Holloway GA. 2010. New substructure filters for removal of pan assay interference compounds (PAINS) from screening libraries and for their exclusion in bioassays. *J Med Chem.* 53:2719–2740.

30 Fedorovich IS, Ganushchak NI, Karpyak VV, Obushchak ND, Lesyuk AI. 2007. Thioamides from 5-arylfurfural and monosubstituted piperazine derivatives (Wilgerodt-Kindler reaction). *Russ J Org Chem.* 43:1190–1195.

31 Bach T, *et al.* 2014. Identification of small molecule NPR-B antagonists by high throughput screening—potential use in heart failure. *Naunyn Schmiedebergs Arch Pharmacol.* 387:5–14.

32 Andresen H, *et al.* 2023. Novel enhancers of guanylyl cyclase-A activity acting via allosteric modulation. *Br J Pharmacol.* 180:3254–3270.

33 Murakami S, *et al.* 2004. C-type natriuretic peptide attenuates bleomycin-induced pulmonary fibrosis in mice. *Am J Physiol Lung Cell Mol Physiol.* 287:L1172–L1177.

34 Hu P, *et al.* 2015. Exogenous C-type natriuretic peptide infusion ameliorates unilateral ureteral obstruction-induced tubulointerstitial fibrosis in rats. *Lab Invest.* 95:263–272.

35 Doyle DD, Upshaw-Earley J, Bell EL, Palfrey HC. 2002. Natriuretic peptide receptor-B in adult rat ventricle is predominantly confined to the nonmyocyte population. *Am J Physiol Heart Circ Physiol.* 282:H2117–H2123.

36 Moyes AJ, *et al.* 2020. C-type natriuretic peptide co-ordinates cardiac structure and function. *Eur Heart J.* 41:1006–1020.

37 Jansen HJ, *et al.* 2019. NPR-C (natriuretic peptide receptor-C) modulates the progression of angiotensin II-mediated atrial fibrillation and atrial remodeling in mice. *Circ Arrhythm Electrophysiol.* 12:e006863.

38 Chen HH, *et al.* 2012. Novel protein therapeutics for systolic heart failure: chronic subcutaneous B-type natriuretic peptide. *J Am Coll Cardiol.* 60:2305–2312.

39 Colucci WS, *et al.* 2000. Intravenous nesiritide, a natriuretic peptide, in the treatment of decompensated congestive heart failure. Nesiritide Study Group. *N Engl J Med.* 343:246–253.

40 Hata N, *et al.* 2008. Effects of carperitide on the long-term prognosis of patients with acute decompensated chronic heart failure: the PROTECT multicenter randomized controlled study. *Circ J.* 72:1787–1793.

41 Hubers SA, *et al.* 2021. B-type natriuretic peptide and cardiac remodelling after myocardial infarction: a randomised trial. *Heart.* 107:396–402.

42 Kitakaze M, *et al.* 2007. Human atrial natriuretic peptide and nicorandil as adjuncts to reperfusion treatment for acute myocardial infarction (J-WIND): two randomised trials. *Lancet.* 370:1483–1493.

43 Wan SH, *et al.* 2016. Chronic peptide therapy with B-type natriuretic peptide in patients with Pre-clinical diastolic dysfunction (stage B heart failure). *JACC Heart Fail.* 4:539–547.

44 Chen HH, *et al.* 2021. First-in-human study of MANP: a novel ANP (atrial natriuretic peptide). analog in human hypertension. *Hypertension.* 78:1859–1867.

45 Kawakami R, *et al.* 2018. A human study to evaluate safety, tolerability, and cyclic GMP activating properties of cenderitide in subjects with stable chronic heart failure. *Clin Pharmacol Ther.* 104:546–552.

46 Savarirayan R, *et al.* 2019. C-type natriuretic peptide analogue therapy in children with achondroplasia. *N Engl J Med.* 381:25–35.

47 Ma X, *et al.* 2023. Evidence for angiotensin II as a naturally existing suppressor for the guanylyl cyclase A receptor and cyclic GMP generation. *Int J Mol Sci.* 24:8547.